

## Grand Challenges of Perovskite and Metal Oxide-based Membrane: A Form of Dual-layer Hollow Fibre

S. D. Nurherdiana<sup>a</sup>, T. Gunawan<sup>b</sup>, N. Widiastuti<sup>b</sup> & H. Fansuri<sup>b\*</sup>

<sup>a</sup>Department of Chemical Engineering, Faculty of Engineering, Universitas Pembangunan Nasional “Veteran” Jawa Timur, Jl. Raya Rungkut Madya Gunung Anyar, Surabaya, East Java, 60294, Indonesia

<sup>b</sup>Department of Chemistry, Faculty of Science and Data Analytics, Institut Teknologi Sepuluh Nopember, Kampus ITS Sukolilo, Surabaya, East Java, 60111, Indonesia

Submitted: 1/4/2021. Revised edition: 15/7/2021. Accepted: 18/7/2021. Available online: 15/11/2021

### ABSTRACT

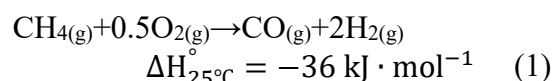
Perovskite and metal oxides-based dual-layer hollow fibre membrane (DHF) has a high appeal as separator and catalyst for methane conversion application which operated at intermediate and high temperature. The membrane mostly fabricated via the co-extrusion followed by co-sintering method, which is quite challenging, due to the complexity to handle the barrier between layers from delamination, membrane cracking and crystal structure distortion which affects the material performance in a DHF form. This recent review clarifies the challenges in the DHF fabrication process to regulate physical and chemical properties in terms of mechanical strength, tightness, elemental distribution, and crystal structure stability. The based material of the membrane focuses on NiO-YSZ in the inner layer directly interconnected with LSCF-YSZ in the outer layer. The understanding of the challenges in DHF fabrication, will further reduce crucial errors in the fabrication process and accelerate performance improvement for application such as syngas, methanol and long-chain hydrocarbons production, and solid oxide fuel cell.

*Keywords:* Perovskite oxide, membrane, methane conversion, dual-layer membrane, membrane fabrication

### 1.0 INTRODUCTION

Natural gas as the future energy perspective is naturally deposited in the world with methane as the main component around 60-90%. However, methane was burned freely by some oil refineries because is incompressible and difficult to distributes [1]. Methane emission to the atmosphere has a very serious impact on greenhouse effect which is 21 times more harmful than carbon dioxide (CO<sub>2</sub>) [2]. Conversion of methane to value added chemicals such as syngas, methanol and long chain hydrocarbons through direct and indirect oxidation reactions. Indirect

oxidation methods such as oxidation partial methane (OPM). The OPM produces syngas under exothermic conditions as shown in Equation 1, thus it reduced operating costs by 30% and can be realized on a large (industrial) and small (laboratory) scale [3].



As shown in the Equation 1, the reaction requires controlled oxygen supplier and a highly compatible catalysts. Among of them, perovskite

\* Corresponding to: H. Fansuri (email: h.fansuri@chem.its.ac.id)  
DOI: <https://doi.org/10.11113/amst.v25n3.217>

oxide has a unique characteristic, namely mixed ionic-electronic conductivity (MIEC) which contributes to the oxygen ion diffusion and electronic conductivity simultaneously through the crystal structure. For instance,  $\text{La}_{0.6}\text{Sr}_{0.4}\text{Co}_{0.2}\text{Fe}_{0.8}\text{O}_{3-\delta}$  (LSCF)-based membrane has attracted more interest for oxygen separator and catalyst for methane conversion [4]. Subsequently, a dual-layer hollow fibre membrane began to be developed in an effort to improve the membrane performance both as simultaneous oxygen separator from air and catalyst, namely NiO-YSZ/LSCF-YSZ [5–8]. Ytria-stabilized zirconia (YSZ) also known to improve the diffusion and conductivity as well as prevent the ionic and electronic block in one side of the membrane [6]. While nickel oxide (NiO) supports the catalytic side in the membrane.

Novel dual-layer hollow fibre membrane for methane conversion which based on LSCF and NiO needs high temperature to initiate the work of active site around 700-1000 °C [9]. Thus, it presents a challenge in

designing high stability in physical and chemical properties, such as compatibility, mechanical strength, tightness, pore configuration, elemental distribution and crystallography identification and effective experiments as illustrated in Figure 1. The figure provides information on the most crucial physical and chemical properties to be focused in the performance development of related membranes, thus the failure can be minimized during fabrication due to a high precision requirement of handling the process.

This article presents the discussion of the challenges during the fabrication of a dual-layer hollow fibre membrane which supported by experience and reports from authors and literatures. This aims to clear the way to design research and perform the optimization in areas related to perovskite and metal oxide based dual-layer hollow fibre membranes for high temperature applications.

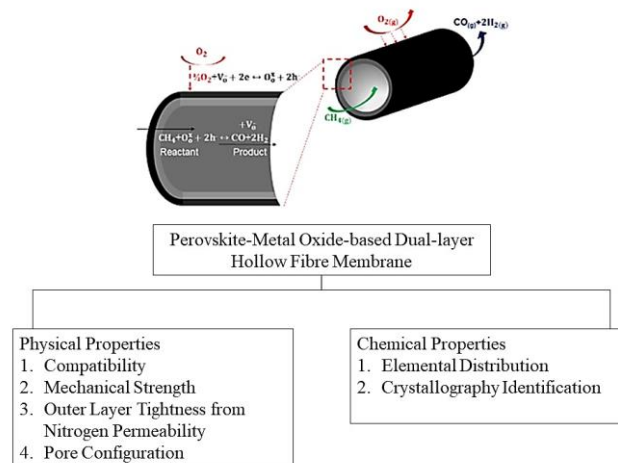


**Figure 1** The Most Crucial Physical and Chemical Properties in Fabricating Dual-Layer Hollow Fibre Membrane for Methane Conversion Application (Nurherdiana *et al.*, 2019)

## 2.0 DISCUSSIONS

This sub-chapter describes in detail the some of the crucial challenges in the

sequence step of membrane fabrication.

### Material Selection for Dual-Layer Hollof Fibre Membrane

Material selection for perovskite and metal oxide is a key aspect in the development of dual-layer hollow fibre membrane, especially for a controlled oxygen reaction application and high temperature.

Perovskites composed of A and B site to form  $ABO_3$  compound, contributes a mixed ionic-electronic conducting (MIEC) property, namely the ability to diffuse oxygen ions ( $O^{2-}$ ) and electrons. simultaneously through

the crystal lattice [10].

The formation of oxygen ions occurs by absorbing electrons from the lattice in membrane. Then the oxygen ions migrate to the other side of the membrane which has a low oxygen pressure. At the same time, the metal ion on the B side of the perovskite is oxidized to a higher valence state by releasing electrons to balance the local charge. The conduction of electrons from the B cation lattice is obtained from the B-O-B bond by means of the Zerner double exchange mechanism as shown in the following reaction:

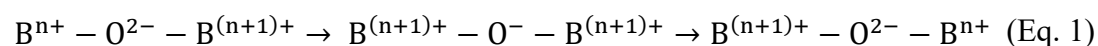


Table 1 shows the perovskite oxide based LSF and their value of resistance, electron and ionic conductivity which contribute on the transfer of oxygen ion and electron through the crystal lattice. Murata *et al.* reported that the resistance value less than  $1.5 \Omega \cdot \text{cm}^2$  contributes high oxygen flux [11]. From the data in Table 1, perovskite oxide based on LSF expected to provide good impact for methane conversion catalysis. In addition, Jiang

*et al.* represented that LSF based perovskite has a good electron conductivity, stability and high electrochemical activity for oxygen reduction at high temperature [12].  $\text{La}_{0.7}\text{Sr}_{0.3}\text{Co}_{0.2}\text{Fe}_{0.8}\text{O}_{3-\delta}$  (LSCF) is a LSF-based perovskite oxide with lower  $\text{CO}_2$  reactivity and improved structural stability compared to other LSFs. Nevertheless, its oxygen flux is still low [13, 14].

**Table 1** Resistance value (R), electron conductivity ( $\delta e$ ) and ion conductivity ( $\delta i$ ) of the perovskite oxides

Perovskite Oxide Materials	Calcination temperature (°C)	R ( $\Omega \cdot \text{cm}^2$ )	$\delta e$ ( $\text{S cm}^{-1}$ )	$\delta i$ ( $\text{S cm}^{-1}$ )	Ref
$\text{La}_{0.6}\text{Sr}_{0.4}\text{Co}_{0.2}\text{Fe}_{0.8}\text{O}_{3-\delta}$	1000	1.36	-	-	[11]
$\text{La}_{0.6}\text{Sr}_{0.4}\text{Co}_{0.2}\text{Fe}_{0.8}\text{O}_{3-\delta}$	850	0.83	-	-	
$\text{La}_{0.6}\text{Sr}_{0.4}\text{Co}_{0.2}\text{Fe}_{0.8}\text{O}_{3-\delta}$	900	0.84	-	-	
$\text{La}_{0.8}\text{Sr}_{0.2}\text{MnO}_3$	900	-	300	$5.93 \times 10^{-7}$	[12]
$\text{La}_{0.6}\text{Sr}_{0.4}\text{Co}_{0.2}\text{Fe}_{0.8}\text{O}_3$	900	-	230	-	
$\text{La}_{0.6}\text{Sr}_{0.4}\text{Co}_{0.8}\text{Fe}_{0.2}\text{O}_3$	900	-	-	0.2	

As previously observed, it is necessary to have a supporting catalyst that increases its effectiveness and performance of the catalytic reaction. Of particular solution is the addition of other material catalyst such as metal

oxide, zeolite and perovskite oxide as represented in Table 2. Metal catalysts such Rh, Ru, Pt, Pd, Ir, Ag, Pt, and Ni have higher catalytic activity and were not easily poisoned by carbon deposition. However, from an

economic point of view, catalyst from metal were expensive [15]. Most of the Nickel, comes from metal oxide NiO which is easier to obtain, has high electron conductivity and is able to increase the selectivity of CO and H<sub>2</sub>. Au *et al.* used a NiO/Al<sub>2</sub>O<sub>3</sub> catalyst at a reaction temperature of 500 °C [16]. Nickel oxide was active in metallic form (oxidation state = 0). The phase

change of metal oxides to metals can be achieved through two different methods, namely i). The reactor is operated at a methane conversion reaction temperature of up to more than 800 °C and ii). Flowing H<sub>2</sub> gas at 500 °C for more than 1 hour on the catalyst surface as reported by Au and Wang [16].

**Table 2** Catalyst for Methane Conversion

Catalyst	Temp (°C)	Time (h)	CH <sub>4</sub> conv (%)	Syngas Selectivity (%)		Ref
				H <sub>2</sub>	CO	
Ni/Al <sub>2</sub> O <sub>3</sub>	900	-	80	-	90	[17]
Ni/MgO	750	100	91.2	96.3	92.4	[18]
Ni-Mg/Al <sub>2</sub> O <sub>3</sub>	800	-	96.5	94	95	[19]
NiO(75)-Al <sub>2</sub> O <sub>3</sub>	650	25	65	80	70	[20]
Ni/zeolit Y	700	89.6	-	88.7		[21]
Mesopori NiO-Al <sub>2</sub> O <sub>3</sub>	600	40	80	76	95	[15]
Ni-zeolit BEA	625-750	4-8	6-7	-	40-50	[22]
Pt/10%Rh	800	8	28.2		94	[23]
Pt-CeO <sub>2</sub>	800	-	98	61	48	[24]
Ag/CGA	600	-	23.4	-	94	[25]

Ni catalyst without supporting material easily triggers local oxidation reactions and is easily deactivated by coking, thus the combination with perovskite is one of the solutions [17, 18, 20, 26, 27]. The problem comes from significantly different thermal expansion coefficient (TEC) between NiO and LSCF at 800-1000 °C of  $14.1 \times 10^{-6} \text{ } ^\circ\text{C}^{-1}$  for NiO while LSCF is  $20.2 \times 10^{-6} \text{ } ^\circ\text{C}^{-1}$  [28]. This difference cause delamination and membrane cracking during the reaction conditions, resulting in a decrease in the performance.

A second way of optimizing the dual-layer membrane is by adding 8% ml yttria-stabilized Zirconia (YSZ) in each layer. YSZ provides good chemical compatibility (stable up to 200 h at 1200 °C and 24 hours at 1400

°C) and thermal expansion coefficient (TEC) of  $3.85 \times 10^{-8} \text{ } ^\circ\text{C}^{-1}$  [17,18,20,26,27]. It automatically prevents the local spot reaction between layer and membrane delamination by modified the TEC value of each layer. In addition, YSZ easily form a matrix connecting between two layers with a strong connection and moderate shrinkage at high temperatures. Currently, research on the ratio and size of particles of perovskite, metal oxide and YSZ is still being carried out.

#### **Fabrication Method: Co-Extrusion followed by Co-sintering**

The co-extrusion method was the most used method to fabricate dual-layer hollow fibre membrane which fully

controlled by the spinneret and syringe pump. The process stage begins with formulating the dope suspension then carrying rheological analysis which based on the Stokes method. Rheology is a technique for measuring the flow of matter, especially solution to ensure the smooth extrusion of the dope suspension. In this study, rheological studies were carried out using a viscosity measurement technique. The viscosity values are recorded at the shear rate from 2 to 60 s<sup>-1</sup> [29].

The viscosity of the suspensions affects the well-extrusion to ensure the stable membrane thickness and diameter. The inner membrane suspension tends to have a greater viscosity than the outer layer suspension which due to achieve stable and strong interconnection between two layers [8, 30]. The main factor affecting the viscosity value is particle size and ratio of the material, especially the powder from perovskite and metal oxide as well as YSZ.

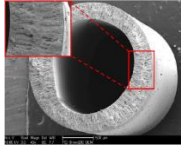
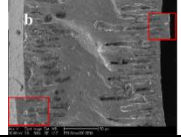
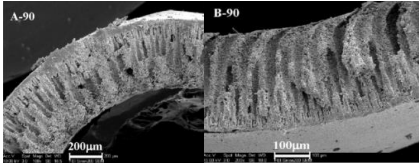
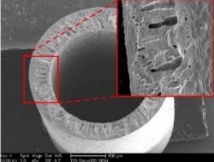
In addition, the extrusion rate also affects the thickness of the membrane, both inner and outer layers. The thinner membrane layer was successfully achieved by applying higher extrusion rate. Consequently, mechanical strength and permeation can be modified by modifying the thickness of the membrane layer [31]. The flow rate of the bore liquid as internal coagulant can affect considerably to the consistency of extruded membrane and pore configuration. Nurherdiana *et al.* [5] successfully explained the effect of different bore liquid composition on the membrane properties, especially the pore configuration. The result showed that a mixed bore liquid achieved asymmetric pore configuration which is desirable for oxygen flux in high temperature. However, it sacrificed the mechanical

strength and affect the membrane to be more brittle.

The asymmetric pore configuration consists of finger-like pores that are directly integrated with sponge-like pores. Yuan *et al.* [32] reported that a finger-like pore provides a route with less resistance for oxygen permeability, while sponge-like contributes to the major mechanical strength and membrane selectivity.

Pore modification was mostly used to be applied for achieving high gas permeability and selective membranes. The affecting parameters was summarized in Table 3 such as internal/external coagulant solution (bore fluid), polymer additives, extrusion flow rate, air gap distance and sintering process. The influencing factors are the addition of polymer additives such as polyethylene glycol (PEG) and polyvinyl chloride (PVP) which more widely used to fabricate ceramic membrane than water, LiCl and ZnCl<sub>2</sub> due to PEG and PVP increase the production of uniform membrane pore configuration [33–36]. Several studies have explained that the value of the molecular weight of the polymer was also sensitive to changes in the pores which affected by the exchange rate between coagulant during immersion process [36–38]. The pores play the important role on the membrane performance, thus the pore consistency during some treatment on the fabrication need to be considered, such as co-sintering temperature.

**Table 3** Effect of Internal Coagulants and Additives on The Morphology and Performance of Hollow Fiber Membranes

Materials	Int/Ext Coagulant	Additive	Reaction Temp (°C)	Mechanical Strength (MPa)	Oxygen Permeation (mL.cm <sup>-2</sup> .min <sup>-1</sup> )	Morphology	Ref
BSCZ <sub>0.05</sub> F	H <sub>2</sub> O/H <sub>2</sub> O	-	950	58.8	4.13		[41]
BSCZ <sub>0.1</sub> F	H <sub>2</sub> O/H <sub>2</sub> O	-		69.8	3.58		
BSCZ <sub>0.2</sub> F	H <sub>2</sub> O/H <sub>2</sub> O	-		84	3.28		
LSF 73	H <sub>2</sub> O/H <sub>2</sub> O	-	950	-	1.4		[42]
LSCF 6428	H <sub>2</sub> O:NMP (A90)/H <sub>2</sub> O	PVP	950	110	1.61		[43]
	Ethanol:NMP (B90)/H <sub>2</sub> O			90	1.89		
	Ethanol/H <sub>2</sub> O			155	0.90		
	H <sub>2</sub> O/H <sub>2</sub> O			155	0.16		
LSCF 6428	Ethanol:NMP (B50)/H <sub>2</sub> O	PVP	950	-	2.60		[13]

Co-sintering based technique was currently well-known to be applied for producing inorganic membrane, especially perovskite-based membrane for high temperature application. The co-sintering method is carried out in stages with dwelling at each temperature of 400-500 °C to remove organic components, then increase it to a final temperature of 1200-1500 °C for 8 hours to complete the co-sintering process [39].

The success of the co-sintering process is based on the tightness of the outer layer of the membrane with a minimum nitrogen leakage value at  $10^{-10} \text{ mol}\cdot\text{m}^{-2}\cdot\text{s}^{-1}\cdot\text{Pa}^{-1}$  as described by Rabuni *et al.* [40] and a membrane mechanical strength of around 400 MPa. Other than that, the chemical properties can also be considered by setting the temperature profile of co-sintering.

It can be evaluated through elemental distribution analysis using scanning electron microscopy-energy dispersive X-ray (SEM-EDX) and crystallography through X-ray diffraction (XRD) analysis. The different elemental compositions in the two layers revealed the analysis of elemental distribution very important which aims to identify membrane formation, as referred to in Sandoval *et al.* [44]. The constituent elements of LSCF were also found to overlap with the Ni signal in the inner layer, as well as yttria and zirconia. However, in the EDX yield estimates, strontium and lanthanum were mostly found in the outer layer of the two-layered membrane without any significant difference.

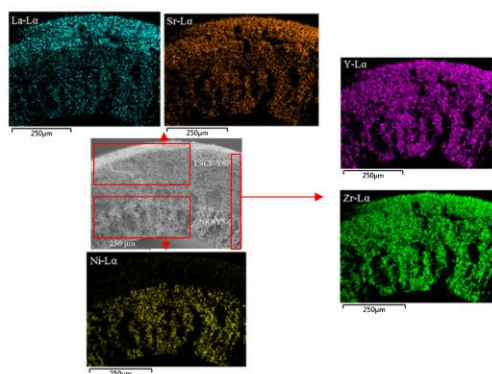


**Figure 1** SEM-EDX result of NiO-YSZ/LSCF-YSZ Dual-layer Hollow Fibre Membrane[5]

Further understanding about the chemical properties of the membrane can be obtained by identifying the phase stability of NiO, YSZ and LSCF. The XRD was applied to record the significant phase changes in each layer (Figure 2). The crystallinity of the phases in the inner and outer layers decreases with increasing temperature of co-sintering. The inner layer phase remains unchanged and there is no impurity phase formation even up to

1500 °C, while the NiO peaks show a larger  $2\theta$  shift. This indicates that the NiO crystal size decreases at the higher sintering temperature. This differs from the diffractogram on the outer membrane layer composed of the LSCF and YSZ composites. At 1400 °C sintering temperature indicates the presence of a secondary phase in the form of  $\text{La}_2\text{Zr}_2\text{O}_7$  (PDF: 00-071-2363) around  $2\theta$ : 28 and 48°.

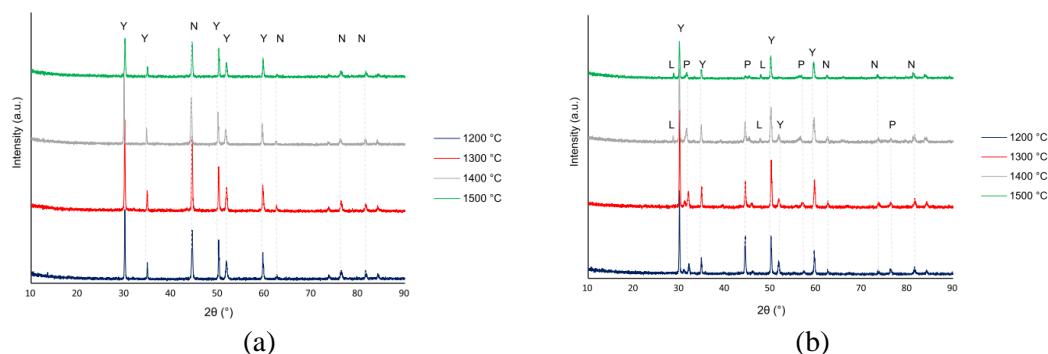


**Figure 2** The XRD Pattern of inner (a) and outer (b) layers of NiO-YSZ/LSCF-YSZ dual-layer Hollow Fibre Membrane [5]. (Y: YSZ, N: Ni, P: LSCF and L:  $\text{La}_2\text{Zr}_2\text{O}_7$ )

Therefore, the sintering temperature at 1300 °C indicates a low level of impurity phase which maintains the stability of the function of the material in the membrane form. The results of research on the chemical properties of the membrane were minimal and incomplete, thus the above explanation was obtained by the authors based on previous report [5].

sintering process. With a better understanding of the correlation between physical and chemical properties, it possible to achieve wider knowledge on the prediction of reaction mechanism and an advanced kinetic study of the DHF for methane conversion at high temperature.

### 3.0 FUTURE OUTLOOK

- A combination of perovskite and metal oxide as the base material in dual-layer hollow fibre can be formed using co-extrusion followed by co-sintering method. The parameter condition can be explored with respect to the physical and chemical properties.
- The physical and chemical properties were crucial to be considered to enhance the performance which due to almost literature mainly focusses on physical properties. Thus, the further identification in the chemical stability involving in-situ monitoring during treatment for membrane fabrication such as the presence of particle collision during mixing in suspension preparation and high temperature in the co-

### ACKNOWLEDGEMENT

The authors would like to thank AMTEC UTM, Johor for providing facilities and guides to finish this project. The authors are also grateful for the funding of the PPKI research scheme with contract No. 1327/PKS/ITS/2021.

### REFERENCES

- [1] S. O. Fakayode, B. S. Mitchell, D. A. Pollard. 2014. Determination of Boiling Point of Petrochemicals by Gas Chromatography-Mass Spectrometry and Multivariate Regression Analysis of Structural Activity Relationship. *Talanta*. 126: 151-156.
- [2] A. M. Fiore, D. J. Jacob, B. D. Field, D. G. Streets, S. D.



- Fernandes, C. Jang. 2002. Linking Ozone Pollution and Climate Change: The Case for Controlling Methane. *Geophys. Res. Lett.* 29: 25-1-25-4.
- [3] F. Pohlmann, A. Jess. 2016. Interplay of Reaction and Pore Diffusion during Cobalt-catalyzed Fischer-Tropsch Synthesis with CO<sub>2</sub>-rich Syngas. *Catal. Today.* 275: 172-182.
- [4] H. Pan, L. Li, X. Deng, B. Meng, X. Tan, K. Li. 2013. Improvement of Oxygen Permeation in Perovskite Hollow Fibre Membranes by the Enhanced Surface Exchange Kinetics. *J. Memb. Sci.* 428: 198-204.
- [5] S. D. Nurherdiana, W. P. Utomo, H. B. N. Sajidah, S. M. Jamil, M. H. D. Othman, H. Fansuri. 2019. Comprehensive Study of Morphological Modification of Dual-Layer Hollow Fiber Membrane. *Arab. J. Sci. Eng.* 44: 10041-10055.
- [6] M. H. D. Othman, N. Drousiotis, Z. Wu, G. Kelsall, K. Li. 2012. Dual-layer Hollow Fibres with Different Anode Structures for Micro-tubular Solid Oxide Fuel Cells. *J. Power Sources.* 205: 272-280.
- [7] T. Li, Z. Wu, K. Li. 2015. Co-extrusion of Electrolyte/anode Functional Layer/Anode Triple-layer Ceramic Hollow Fibres for Micro-tubular Solid Oxide Fuel Cells-electrochemical Performance Study. *J. Power Sources.* 273: 999-1005.
- [8] M. H. Mohamed, M. H. D. Othman, A. M. Mutalib, M. Rahman, J. Jaafar, A. F. Ismail, M. I. H. M. Dzahir. 2016. Structural Control of NiO-YSZ/LSCF-YSZ Dual-Layer Hollow Fiber Membrane for Potential Syngas Production. *Int. J. Appl. Ceram. Technol.* 13: 799-809.
- [9] Z. Wu, B. Wang, K. Li. 2011. Functional LSM-ScSZ/NiO-ScSZ Dual-layer Hollow Fibres for Partial Oxidation of Methane. *Int. J. Hydrogen Energy.* 36: 5334-5341.
- [10] A. Möbius, D. Henriques, T. Markus. 2009. Sintering behaviour of La<sub>1-x</sub>Sr<sub>x</sub>Co<sub>0.2</sub>Fe<sub>0.8</sub>O<sub>3-δ</sub> (0.3 ≤ x ≤ 0.8) Mixed Conducting Materials. *J. Eur. Ceram. Soc.* 29: 2831-2839.
- [11] K. Murata, T. Fukui, H. Abe, M. Naito, K. Nogi. 2005. Morphology Control of La(Sr)Fe(Co)O<sub>3-α</sub> Cathodes for IT-SOFCs. *J. Power Sources.* 145: 257-261.
- [12] S. P. Jiang. 2002. A Comparison of O<sub>2</sub> Reduction Reactions on Porous (La,Sr)MnO<sub>3</sub> and (La,Sr)(Co,Fe)O<sub>3</sub> Electrodes. *Solid State Ionics.* 146: 1-22.
- [13] X. Tan, N. Liu, B. Meng, J. Sunarso, K. Zhang, S. Liu. 2012. Oxygen Permeation Behavior of La<sub>0.6</sub>Sr<sub>0.4</sub>Co<sub>0.8</sub>Fe<sub>0.2</sub>O<sub>3</sub> Hollow Fibre Membranes with Highly Concentrated CO<sub>2</sub> Exposure. *J. Memb. Sci.* 389: 216-222.
- [14] H. Wang, Y. Cong, W. Yang. 2002. Oxygen Permeation Study in a Tubular Ba<sub>0.5</sub>Sr<sub>0.5</sub>Co<sub>0.8</sub>Fe<sub>0.2</sub>O<sub>3-δ</sub> Oxygen Permeable Membrane. *J. Memb. Sci.* 210: 259-271.
- [15] C. Ding, W. Liu, J. Wang, P. Liu, K. Zhang, X. Gao, G. Ding, S. Liu, Y. Han, X. Ma. 2015. One Step Synthesis of Mesoporous NiO – Al<sub>2</sub>O<sub>3</sub> Catalyst for Partial Oxidation of Methane to Syngas: The Role of Calcination Temperature. *FUEL.* 162: 148-154.
- [16] C. T. Au, H. Y. Wang. 1996. Pulse Study of Methane Partial Oxidation to Syngas Over SiO<sub>2</sub>-

- Supported Nickel Catalysts, *Catal. Letters*. 41: 159-163.
- [17] D. Dissanayake, M. P. Rosynek, K. C. C. Kharas, J. H. Lunsford. 1991. Partial Oxidation of Methane to Carbon Monoxide and Hydrogen over a Ni/Al<sub>2</sub>O<sub>3</sub> Catalyst. *J. Catal.* 132: 117-127.
- [18] S. Tang, J. Lin, K. Tan. 1998. Partial Oxidation of Methane to Syngas over Ni/MgO, Ni/CaO and Ni/CeO<sub>2</sub>. *Catal. Letters*. 51: 169-175.
- [19] K. M. Lee, W. Y. Lee. 2002. Partial Oxidation of Methane to Syngas over Calcined Ni-Mg/Al Layered Double Hydroxides, *Catal. Letters*. 83: 65-70.
- [20] Y. Kobayashi, J. Horiguchi, S. Kobayashi, Y. Yamazaki, K. Omata, D. Nagao, M. Konno, M. Yamada. 2011. Effect of NiO Content in Mesoporous NiO-Al<sub>2</sub>O<sub>3</sub> Catalysts for High Pressure Partial Oxidation of Methane to Syngas. *Appl. Catal. A Gen.* 395: 129-137.
- [21] A. Mosayebi, R. Abedini. 2014. Partial Oxidation of Butane to Syngas using Nano-structure Ni/zeolite Catalysts. *J. Ind. Eng. Chem.* 20: 1542-1548.
- [22] I. Rossetti, M. Compagnoni, E. Finocchio, G. Ramis, A. Di Michele, A. Zucchini, S. Dzwigaj. 2016. Syngas Production via Steam Reforming of Bioethanol over Ni-BEA Catalysts: A BTL Strategy. *Int. J. Hydrogen Energy*. 41: 16878-16889.
- [23] K. Hofstad, T. Sperle, O. Rokstad, A. Holmen. 1997. Partial Oxidation of Methane to Synthesis Gas over a Pt/10% Rh Gauze. *Catal. Letters*. 45: 97-105.
- [24] W. Tang, Z. Hu, M. Wang, G. D. Stucky, H. Metiu, E. W. McFarland. 2010. Methane Complete and Partial Oxidation Catalyzed by Pt-doped CeO<sub>2</sub>. *J. Catal.* 273: 125-137.
- [25] E. Ruiz-Trejo, P. Boldrin, J. L. Medley-Hallam, J. Darr, A. Atkinson, N. P. Brandon. 2015. Partial Oxidation of Methane Using Silver/Gadolinia-doped Ceria Composite Membranes, *Chem. Eng. Sci.* 127: 269-275.
- [26] W. He, J. Liu, C. Chen, M. Ni. 2015. Oxygen Permeation Modeling for Zr<sub>0.84</sub>Y<sub>0.16</sub>O<sub>1.92</sub>-La<sub>0.8</sub>Sr<sub>0.2</sub>Cr<sub>0.5</sub>Fe<sub>0.5</sub>O<sub>3-δ</sub> Asymmetric Membrane Made by Phase-inversion. *J. Memb. Sci.* 491: 90-98.
- [27] H. Özdemir, M. A. Faruk Öksüzömer, M. Ali Gürkaynak. 2010. Preparation and Characterization of Ni based Catalysts for the Catalytic Partial Oxidation of Methane: Effect of Support Basicity on H<sub>2</sub>/CO Ratio and Carbon Deposition. *Int. J. Hydrogen Energy*. 35: 12147-12160.
- [28] H. Fansuri, M. I. Syafi'i, S. Romdoni, A. D. Masyitoh, W. P. Utomo, D. Prasetyoko, N. Widiastuti, I. K. Murwani, Subaer. 2017. Preparation of Dense Ba<sub>x</sub>Sr<sub>1-x</sub>Co<sub>0.8</sub>Fe<sub>0.2</sub>O<sub>3</sub> Membranes: Effect of Ba<sup>2+</sup> Substituents and Sintering Method to the Density, Hardness and Thermal Expansion Coefficient of the Membranes. *Adv. Mater. Lett.* 8: 799-806.
- [29] R. Fernández-González, T. Molina, S. Savvin, R. Moreno, A. Makradi, P. Núñez. 2014. Characterization and Fabrication of LSCF Tapes. *J. Eur. Ceram. Soc.* 34: 953-959.
- [30] S. H. Ahmad, S. M. Jamil, M. H. D. Othman, M. A. Rahman, J. Jaafar, A. F. Ismail. 2017. Co-extruded Dual-layer Hollow Fiber with Different Electrolyte

- Structure for a High Temperature Micro-tubular Solid Oxide Fuel Cell. *Int. J. Hydrogen Energy*. 42: 9116-9124.
- [31] M. H. D. Othman, N. Droushiotis, Z. Wu, K. Kanawka, G. Kelsall, K. Li. 2010. Electrolyte Thickness Control and Its Effect on Electrolyte/Anode Dual-layer Hollow Fibres for Micro-tubular Solid Oxide Fuel Cells. *J. Memb. Sci.* 365: 382–388.
- [32] R. hua Yuan, W. He, Y. Zhang, J. F. Gao, C. sheng Chen. 2016. Preparation and Characterization of Supported Planar  $Zr_{0.84}Y_{0.16}O_{1.92}$ - $La_{0.8}Sr_{0.2}Cr_{0.5}Fe_{0.5}O_{3-\delta}$  Composite Membrane. *J. Memb. Sci.* 499: 335-342.
- [33] M. H. Zare, N. Hajilary, M. Rezakazemi. 2019. Microstructural Modifications of Polyethylene Glycol Powder Binder in the Processing of Sintered Alpha Alumina Under Different Conditions of Preparation. *Mater. Sci. Energy Technol.* 2: 89-95.
- [34] N. N. Aminudin, H. Basri, Z. Harun, M. Z. Yunos, G. P. Sean. 2013. Comparative Study on Effect of PEG and PVP as Additives on Polysulfone (PSF) Membrane Structure and Performance. *J. Teknol. (Sciences Eng)*. 65: 47-51.
- [35] X. Tan, S. Liu, K. Li. 2001. Preparation and Characterization of Inorganic Hollow Fiber Membranes. *J. Memb. Sci.* 188: 87-95.
- [36] S. Mansur, M. Hafiz, D. Othman, A. Fauzi, M. Nidzhom, Z. Abidin, N. Said, P. Sean, H. Hasbullah, S. Hamimah, S. Abdul. 2018. Study on the Effect of PVP Additive on the Performance of PSf/PVP Ultrafiltration Hollow Fiber Membrane. 14: 343-347.
- [37] M. Wu, C. Gao, J. Zhang, J. Ma, F. Shi, Y. Ma. 2011. Effect of PEG Additive on the Morphology and Performance of Polysulfone Ultrafiltration Membranes. *Desalination*. 272: 51-58.
- [38] B. Chakrabarty, A. K. Ghoshal, M. K. Purkait. 2008. Effect of Molecular Weight of PEG on Membrane Morphology and Transport Properties. *J. Memb. Sci.* 309: 209-221.
- [39] S. D. W. I. Nurherdiana, R. Etriana, R. M. Iqbal, W. P. Utomo, H. Fansuri. 2019. Effect of the Sintering Process on the Morphology and Flat Membranes Prepared by the Phase Inversion Method. 63: 305-314.
- [40] M. F. Rabuni, T. Li, P. Punmeechao, K. Li. 2018. Electrode Design for Direct-methane Micro-tubular Solid Oxide Fuel Cell (MT-SOFC). *J. Power Sources*. 384: 287-294.
- [41] X. Meng, N. Yang, B. Meng, X. Tan, Z. F. Ma, S. Liu. 2011. Zirconium Stabilized  $Ba_{0.5}Sr_{0.5}(Co_{0.8-x}Zr_x)Fe_{0.2}O_{3-\delta}$  Perovskite Hollow Fibre Membranes for Oxygen Separation. *Ceram. Int.* 37: 2701-2709.
- [42] X. Tan, L. Shi, G. Hao, B. Meng, S. Liu. 2012.  $La_{0.7}Sr_{0.3}FeO_{3-\alpha}$  Perovskite Hollow Fiber Membranes for Oxygen Permeation and Methane Conversion. *Sep. Purif. Technol.* 96: 89-97.
- [43] X. Tan, N. Liu, B. Meng, S. Liu. 2011. Morphology Control of the Perovskite Hollow Fibre Membranes for Oxygen Separation using Different Bore

- Fluids. *J. Memb. Sci.* 378: 308-318.
- [44] M. V. Sandoval, A. Matta, T. Matencio, R. Z. Domingues, G. A. Ludwig, M. De Angelis Korb, C. De Fraga Malfatti, P. Gauthier-Maradei, G. H. Gauthier. 2014. Barium-modified NiO-YSZ/NiO-GDC Cermet as New Anode Material for Solid Oxide Fuel Cells (SOFC). *Solid State Ionics*. 261: 36-44.